2015

Multilevel sequence detection for dynamic mode atomic force microscopy

Yan Ren
Iowa State University

Multilevel sequence detection for dynamic mode atomic force microscopy

by

Yan Ren

A thesis submitted to the graduate faculty

in partial fulfillment of the requirements for the degree of

MASTER OF SCIENCE

Major: Electrical Engineering

Program of Study Committee:

Aditya Ramamoorthy, Major Professor

Dan Nordman

Zhengdao Wang

Iowa State University

Ames, Iowa

2015

TABLE OF CONTENTS

LIST OF FIGURES

ACKNOWLEDGEMENTS

I would like to take this opportunity to express my thanks to those who helped me with various aspects of conducting research and the writing of this thesis. First and foremost, Dr. Aditya Ramamoorthy for his guidance, patience and support throughout this research and the writing of this thesis. His insights and words of encouragement have often inspired me and renewed my hopes for completing my graduate education. I would also like to thank my committee members for their efforts and contributions to this work: Dr. Dan Nordman and Dr. Zhengdao Wang.

ABSTRACT

The atomic force microscope is an instrument that is widely used in fields such as biology, chemistry and medicine for imaging at the atomic level. In this work, we consider a specific mode of AFM usage, known as the dynamic mode where the AFM cantilever probe is forced sinusoidally. In the absence of interaction with the sample being imaged, the cantilever follows a predictable sinusoidal trajectory. The deflection of the cantilever probe changes when it interacts with the sample being imaged and imaging is performed by interpreting these changes.

In this work, we present a sequence detection based algorithm that allows for resolving topographic features into one of three possible levels at a fast speed. We demonstrate the effectiveness of our algorithm via simulation results and by comparing it to a lower bound that is obtained by considering a genie aided detector.

CHAPTER 1. INTRODUCTION

The atomic force microscope (AFM)) [1] is an instrument that is widely used in several areas for imaging at the atomic scale. Fig. 1.1 shows the schematic of an AFM setup. The AFM consists of a cantilever probe that has a sharp tip on one end and is supported on the other end on a cantilever base. The cantilever tip deflects in response to minute atomic level forces that come into play when the tip interacts with a sample. Interpreting the cantilever deflection in an appropriate manner yields the image of the sample. Fig. 1.1 also shows a mechanism for measuring the cantilever deflection signal by means of a photodiode arrangement.

There are two main modes in which the AFM is used. In the static mode, the AFM is in constant contact with the sample. In the dynamic mode operation, the cantilever base is forced sinusoidally by a dither piezo. In the absence of any interaction, the cantilever tip follows a sinusoidal trajectory. However, when the tip interacts with the sample, the trajectory changes. Imaging is performed by interpreting the changes in this deflection signal. The dynamic mode is a significantly gentler mode of operation as the sample is not in constant contact with the medium. We exclusively work with the dynamic mode in our work.

With some analysis and approximation[3], the standard AFM setup (see Fig. 1.1) can be viewed as a block system diagram (see Fig. 1.2) which is composed of linear system G that models the cantilever system when it is oscillating freely, i.e., in the absence of interaction with the sample. When the cantilever starts interacting with the medium, it experiences nonlinear forces, that are modeled by the block ϕ in the feedback loop in

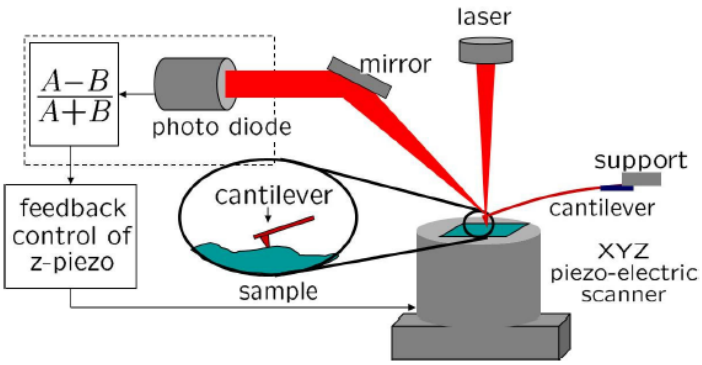

Figure 1.1: The atomic force microscope [2].

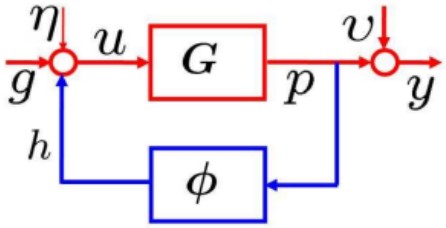

Figure 1.2: The system diagram.[4].

Fig. 1.2. Fig. 1.2 also depicts the sinusoidal dither forcing g, the process noise η and measurement noise v. The position of the cantilever is depicted by p and the nonlinear tip-media force is denoted by h.

Kumar *et al.* introduced and demonstrated in [4] that the AFM setup shown in Fig. 1.1 can be modeled as a communication system (see Fig. 1.3). In this system the feedback loop is broken by modeling the nonlinearity block as a Markov model. However, the parameters of nonlinearity block are assumed to be unknown. Kumar *et al.* obtained these parameters by training data. And based on this system (see Fig. 1.3), two-level sequences (samples with two different topographic profile heights) were detected via the Viterbi algorithm. Profile heights of samples in [4] are assumed to be either *high* or *low*. Here, high profile implies the tip-media interaction between the cantilever and the sample, while low profile indicates no the tip-media interaction.

The scheme proposed in [4] exhibits much better performance than the other detectors developed previously for this problem. A natural extension of this approach would

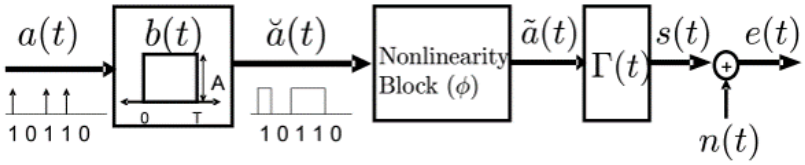

Figure 1.3: The Communication System.[4].

be to attempt to perform higher resolution imaging, e.g., three or four level imaging. However, in our experiments, we have demonstrated that the performance of this approach degrades rapidly when there are more than two levels. In this work, we explore the problem of imaging with a 3-level resolution, i.e., instead of two levels, we consider classifying each feature into one of three possible levels.

Differing from the method proposed by Kumar *et al.* where parameters are trained from data, we assume that all system parameters are known. We emphasize that even when the parameters are known, the problem of detecting the features is rather nontrivial, owing to the nonlinearity ϕ in the feedback loop. Though our proposed algorithm is suboptimal, the performance of our scheme is superior to that of Kumar *et al.* We also present a genie aided detector for determining a meaningful lower bound on the performance of any detector.

This thesis is organized as follows. Section 2, discusses the relevant background and outlines the model under consideration. Section 3, derives the maximum-likelihood function and proposes a greedy algorithm for detection. Section 4 explains the simulation procedure and shows the results. Section 5, outlines the conclusions and opportunities for future work.

CHAPTER 2. BACKGROUND AND MODEL

We model the AFM operation as a communication channel system with feedback as shown in Fig. 2.1. This system comes from the block diagram shown in Fig. 1.2. In particular, we assume that the original continuous time system has been sampled at a high enough rate $1/T_s$. In this system, $g(t)$ represents the dither force which actuates the cantilever in AFM. And $g(t) = A\sin(2\pi t/T_c)$ is a sinusoidal signal with period T_c and amplitude A. Here, T_c is the duration of every cantilever cycle. In each cantilever cycle, the cantilever hits the sample at most once. $\Gamma(t)$ approximates the impulse response of the cantilever system in the absence of any tip-media interaction. We model the response $\Gamma(t)$ as

$$\Gamma(t) = \exp(-\frac{w_c}{2Q}t)\sin(wt)/w \tag{2.1}$$

where Q is the quality factor, $w = w_c\sqrt{1-\frac{1}{4Q^2}}$ and $w_c = 2\pi f_c$ with f_c being the first resonant frequency of the cantilever. Note that the cantilever oscillation period $T_c = 1/f_c$. According to (2.1), the envelope of $\Gamma(t)$ attenuates exponentially with the time and converges towards zero. We denote the tip deflection of the cantilever by $p(t)$. Define input sequence

$$z(t) \triangleq \sum_{k=0}^{N-1} a_k b(t-kT) \tag{2.2}$$

where the rectangular function $b(t) \triangleq \begin{cases} B, & 0 \le t < T \\ 0, & \text{otherwise} \end{cases}$, T is the duration of each feature and a_k takes value in $\{0,1,2\}$ with equal probability for $k = 0, 1, \cdots, N-1$. Here, $a_k = 0$, 1 and 2 represent the height of the sample profile being *low*, *medium* and *high*,

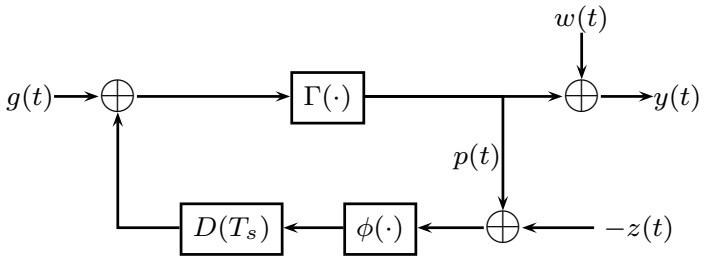

Figure 2.1: System diagram with delay.

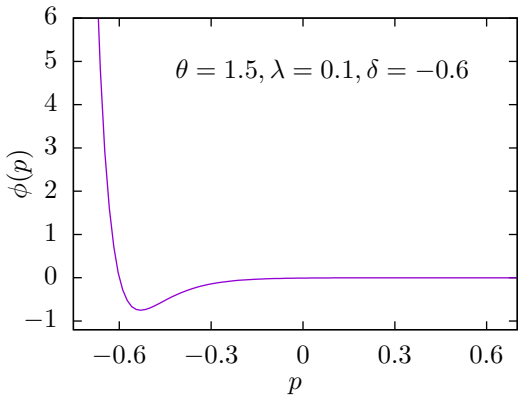

Figure 2.2: The nonlinear tip-media interaction force $\phi(p)$.

respectively. $\phi(\cdot)$ denotes the nonlinear tip-media interaction force with a exponential form which satisfies

$$\phi(p) = 2\theta\left[\left(\mathrm{e}^{-(p-\delta)/\lambda} - \frac{1}{2}\right)^2 - \frac{1}{4}\right] \tag{2.3}$$

where θ, λ and δ are constants that depend on the cantilever and the material properties of the medium being imaged. The plot of $\phi(p)$ shown on Fig. 2.2. The diagram in Fig. 2.1 suggests that the tip-media interaction force ϕ depends on the tip deflection p and is followed by delay of T_s, which is usually one sampling period as needed while discretize the continuous system. Therefore, the tip deflection of the cantilever can be written as

$$p(t) = \Gamma(t) * \Big(g(t) + \phi\big(p(t - T_s) - z(t - T_s)\big)\Big) \tag{2.4}$$

where $*$ represents convolution. The eventual measurements are assumed to be contaminated by the additive white Gaussian noise $w(t)$.

In the discrete implementation, we assume that the cantilever oscillation period $T_c = LT_s$, the duration of each feature $T = qT_c = qLT_s$. Here, $T = qT_c$ implies that the cantilever hits the sample at most q times in each feature duration.

With this signal system model, our goal is to distinguish different height levels of samples by decoding the input sequence $z(t)$, i.e., $\boldsymbol{a} = [a_0, a_1, \cdots, a_{N-1}]^T$ given the output $y(t)$. Due to the nonlinear tip-media interaction (the feedback part in the system), the decoding problem is is quite nontrivial, even though we assume that the system parameters are known. Accordingly, we need to make some assumptions.

Assumption 1 *The effective support of* $\Gamma(t)$ *is limited to be* $[0, r]$ *with* $r = mqL + 1$, *where* $m > 0$ *is an integer.*

At time $t = nT_s$, the discrete form of input sequence $z(t)$ and the output $y(t)$ are $z(nT_s) = z[n] = \sum_{k=0}^{N-1} a_k b\left[(n - kqL)\, T_s\right]$, $y(nT_s) = y[n] = p(nT_s) + w(nT_s) = p[n] + w[n]$, respectively, where $p[n]$ is

$$\begin{aligned} p[n] &= \Gamma[n] * g[n] + \Gamma[n] * 2\theta\left[\left(\mathrm{e}^{-\frac{1}{\lambda}(p[n-1]-z[n-1]-\delta)} - \frac{1}{2}\right)^2 - \frac{1}{4}\right] \\ &= \Gamma[n] * g[n] + 2\theta \sum_{j=0}^{r-1} \Gamma[j]\left[\left(\mathrm{e}^{-\frac{1}{\lambda}(p[n-j-1]-\sum_{k=0}^{N-1} a_k b[n-j-1-kqL]-\delta)} - \frac{1}{2}\right)^2 - \frac{1}{4}\right] \end{aligned} \tag{2.5}$$

Since $b[n] = B$ for $n = 0, 1, \cdots, qL - 1$, $p[n]$ can be simplified as

$$p[n] = \sum_{j=0}^{r-1} \Gamma[j]\left\{g[n-j] + 2\theta\left[\left(\mathrm{e}^{-\frac{1}{\lambda}(p[n-j-1]-BA(n-j)-\delta)} - \frac{1}{2}\right)^2 - \frac{1}{4}\right]\right\} \tag{2.6a}$$

where

$$A(n-j) = \sum_{n-j-1-kqL \in \{0,1,\ldots,qL-1\}} a_k \tag{2.6b}$$

Obviously, k in (2.6b) are integers from $\left\lceil \frac{n-j}{qL} \right\rceil - 1$ to $\left\lfloor \frac{n-j-1}{qL} \right\rfloor$.

Let $\boldsymbol{p}_t = \left[p[tqL+1], \cdots, p[(t+1)qL]\right]^T$, (2.6) implies that $\boldsymbol{p}_t$ relies on $a_{t-m}, \cdots, a_t$ and $p[(t-m)qL], \cdots, p[tqL]$. The t-th feature in the input sequence $\boldsymbol{a}$ has an affect on the measurements $\boldsymbol{y}_t = \left[y[tqL+1], \cdots, y[(t+1)qL]\right]^T$. Note that $\boldsymbol{y}_t = \boldsymbol{p}_t$ in a noise free case.

CHAPTER 3. MAXIMUM-LIKELIHOOD SEQUENCE DETECTION

In this section,we discuss the detection strategy for our proposed model. Since the output $y[n] = p[n] + w[n]$ where $w[n]$ is the white Gaussian noise and every feature in the input sequence $\boldsymbol{a}$ is with equal probability, the maximum-likelihood (ML) sequence detection can be applied. We denote the ML estimate of the input sequence $\boldsymbol{a}_0^{N-1}$ by the sequence $\hat{\boldsymbol{a}}_0^{N-1} = [\hat{a}_0, \hat{a}_1, \cdots, \hat{a}_{N-1}]^T$ that maximizes the conditional probability density function (pdf), i.e.,

$$\hat{\boldsymbol{a}}_0^{N-1} = \arg\max_{\boldsymbol{a}_0^{N-1}} f\left(\boldsymbol{y}_0^{N-1} | \boldsymbol{a}_0^{N-1}\right) \tag{3.1}$$

where

$$\begin{aligned} \boldsymbol{y}_0^{N-1} &= \left[y\left[1\right], \cdots, y\left[qL\right], \cdots, y\left[(N-1)\,qL\right], \cdots, y\left[NqL\right]\right]^T \\ &= \left[\boldsymbol{y}_0^T, \cdots, \boldsymbol{y}_{N-1}^T\right]^T \end{aligned} \tag{3.2}$$

The conditional pdf of $\boldsymbol{y}_0^{N-1}$ given the entire input sequence can be factored as

$$\begin{aligned} f(\boldsymbol{y}_0^{N-1} | \boldsymbol{a}_0^{N-1}) &= f(\boldsymbol{y}_0, \cdots, \boldsymbol{y}_{N-1} | \boldsymbol{a}_0^{N-1}) \\ &= f(\boldsymbol{y}_0, \cdots, \boldsymbol{y}_{N-2} | a_0^{N-1}) f(\boldsymbol{y}_{N-1} | \boldsymbol{y}_0^{N-2}, \boldsymbol{a}_0^{N-1}) && \text{(3.3a)} \\ &= f(\boldsymbol{y}_0, \cdots, \boldsymbol{y}_{N-2} | a_0^{N-2}) f(\boldsymbol{y}_{N-1} | \boldsymbol{y}_0^{N-2}, \boldsymbol{a}_0^{N-1}) && \text{(3.3b)} \\ &\quad \cdots \\ &= f(\boldsymbol{y}_0 | a_0) \prod_{t=1}^{N-1} f(\boldsymbol{y}_t | \boldsymbol{y}_0^{t-1}, \boldsymbol{a}_0^t) && \text{(3.3c)} \end{aligned}$$

As the conditional pdf of $\boldsymbol{y}_t$ shown on function (3.3c) depends on the entire past output $\boldsymbol{y}_0^{t-1}$ and the entire past input sequence $\boldsymbol{a}_0^t$, it appears that the decoding complexity of is

exponential in the sequence length. However, we know that $\boldsymbol{p}_0^t$ depends on $\boldsymbol{a}_0^t$, so certain simplifications are possible. So, the conditional pdf of $\boldsymbol{y}_0^{N-1}$ given $\boldsymbol{a}_0^{N-1}$ can be rewritten as

$$\begin{aligned} f(\boldsymbol{y}_0^{N-1}|\boldsymbol{a}_0^{N-1}) &= f(\boldsymbol{y}_0|a_0)\prod_{t=1}^{N-1} f(\boldsymbol{y}_t|\boldsymbol{y}_0^{t-1},\boldsymbol{a}_0^t) \\ &= f(\boldsymbol{y}_0|a_0)\prod_{t=1}^{N-1} f(\boldsymbol{y}_t|\boldsymbol{y}_0^{t-1},\boldsymbol{p}_0^{t-1},\boldsymbol{a}_0^t) \end{aligned} \tag{3.4}$$

Compared with function (3.3c), $\boldsymbol{p}_0^{t-1}$ is added to function (3.4). The additional information of $\boldsymbol{p}_0^{t-1}$ provides us an opportunity to further simplify the conditional pdf $f(\boldsymbol{y}_t|\boldsymbol{y}_0^{t-1},\boldsymbol{a}_0^t)$ and then obtain a practical detection strategy for the sequence detection.

Before simplifying the pdf function (3.4) further, we introduce the concept of *d*-connection from the literature on graphical models [5].

Definition 1 (*d*-connection) *Let i and j be distinct vertices of a directed acyclic graph (DAG) and Q be a set of vertices not containing i or j. Then, i and j are d-connected given Q if there is an undirected path P between i and j such that*

(i) every collider in P has a descendant in Q, and

(ii) no other vertex [besides possibly those mentioned in (i)] on P is in Q.

And if i and j are not d-connected given Q, they are d-separated given Q.

In Definition 1, a collider is a node c on a given path P with neighbours a and b on P such that $a \to c \leftarrow b$.

Fig. 3.1 is the dependency graph illustrating the relationship between $\boldsymbol{a}, \boldsymbol{p}$ and $\boldsymbol{y}$. We can use this figure to explain the subsequent simplification. In the conditional pdf function $f(\boldsymbol{y}_t|\boldsymbol{y}_0^{t-1},\boldsymbol{p}_0^{t-1},\boldsymbol{a}_0^t)$, $\boldsymbol{y}_0^{t-1}$, $\boldsymbol{p}_0^{t-1}$ and $\boldsymbol{a}_0^{t-1}$ can be respectively represented as

$$\boldsymbol{y}_0^{t-1}=\left[y_0^{(t-m)qL-1}, y_{(t-m)qL}^{tqL}\right]^T, \boldsymbol{p}_0^{t-1}=\left[p_0^{(t-m)qL-1}, p_{(t-m)qL}^{tqL}\right]^T, \boldsymbol{a}_0^{t-1}=\left[\boldsymbol{a}_0^{t-m-1}, \boldsymbol{a}_{t-m}^t\right].$$

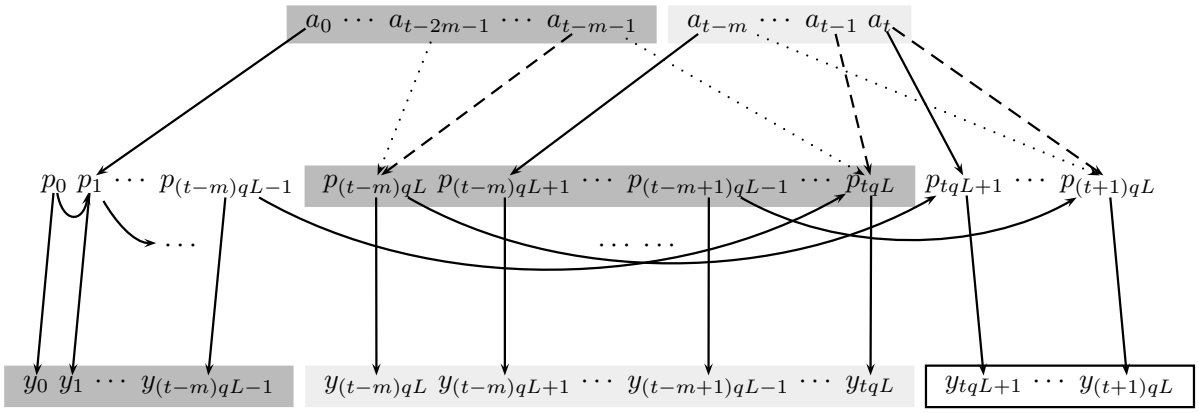

Figure 3.1: Dependency graph for the model.

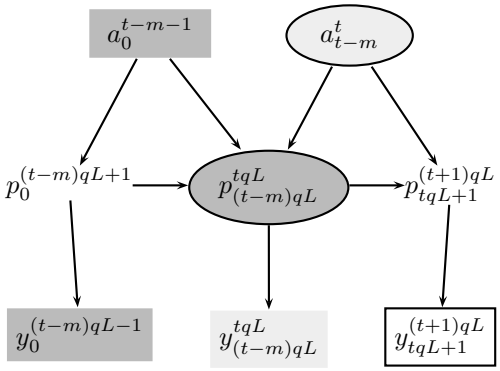

Figure 3.2: Dependence path.

$y_0^{(t-m)qL-1} = \left[y\left[0\right], \cdots, y\left[(t-m)qL-1\right]\right]^T$ and $y_{(t-m)qL}^{tqL} = \left[y\left[(t-m)qL\right], \cdots, y\left[tqL\right]\right]^T$ are two vectors with length $(t-m)qL$ and $mqL+1$ respectively. With these notations, the conditional pdf of $\boldsymbol{y}_t$ given $\boldsymbol{y}_0^{t-1}, \boldsymbol{p}_0^{t-1}, \boldsymbol{a}_0^t$ can be described as,

$$f\left(\boldsymbol{y}_t|\boldsymbol{y}_0^{t-1}, \boldsymbol{p}_0^{t-1}, \boldsymbol{a}_0^t\right) = f\Big(\boldsymbol{y}_t|y_0^{(t-m)qL-1}, y_{(t-m)qL}^{tqL}, p_0^{(t-m)qL-1}, p_{(t-m)qL}^{tqL}, \boldsymbol{a}_0^{t-m-1}, \boldsymbol{a}_{t-m}^t\Big) \tag{3.5}$$

Now we attempt to drop some terms in the conditioning based on identifying appropriate conditional independence relationships by using ideas from graphical models. For this purpose we construct a simplified dependency path graph of relevant quantities which is shown on Fig. 3.2. Given the definition of *d-conneceted* and Fig. 3.2, it is easy to clarify the relationship between $\boldsymbol{y}_t$ and its conditional terms. Let i denote $\boldsymbol{y}_t$, j denote $y_0^{(t-m)qL-1}$, $y_{(t-m)qL}^{tqL}$, $p_0^{(t-m)qL-1}$, or $\boldsymbol{a}_0^{t-m-1}$ and Q denote $p_{(t-m)qL}^{tqL}$ and $\boldsymbol{a}_{t-m}^t$. Given

Q, the vertices $p_{(t-m)qL}^{tqL}$ which are in Q are always on the undirected path P between i and j (as shown in Fig. 3.2). According to the definition of the$d$-connection, i and j don't satisfy the requirement of being d-connected. Thus, i and j are d-separated given Q. Therefore, we can conclude that $\boldsymbol{y}_t$ and $y_0^{(t-m)qL-1}$, $y_{(t-m)qL}^{tqL}$, $p_0^{(t-m)qL-1}$, $\boldsymbol{a}_0^{t-m-1}$ are independent given $p_{(t-m)qL}^{tqL}$ and $\boldsymbol{a}_0^{t-m-1}$. And the conditional pdf of $\boldsymbol{y}_t$ given $\boldsymbol{y}_0^{t-1}$ and $\boldsymbol{a}_0^t$ can be rewritten as

$$\begin{aligned} f\left(\boldsymbol{y}_t|\boldsymbol{y}_0^{t-1},\boldsymbol{a}_0^t\right) &= f\left(\boldsymbol{y}_t|\boldsymbol{y}_0^{t-1},\boldsymbol{p}_0^{t-1},\boldsymbol{a}_0^t\right) \\ &= f\Big(\boldsymbol{y}_t|p_{(t-m)qL}^{tqL},\boldsymbol{a}_{t-m}^t\Big). \end{aligned} \tag{3.6}$$

Using function (3.6), the conditional pdf $f(\boldsymbol{y}_0^{N-1}|\boldsymbol{a}_0^{N-1})$ used for ML sequence detection can be further expressed as

$$\begin{aligned} f(\boldsymbol{y}_0^{N-1}|\boldsymbol{a}_0^{N-1}) &= f(\boldsymbol{y}_0|a_0)\prod_{t=1}^{N-1} f(\boldsymbol{y}_t|\boldsymbol{y}_0^{t-1},\boldsymbol{a}_0^t) \\ &= f(\boldsymbol{y}_0|a_0)\prod_{t=1}^{N-1} f(\boldsymbol{y}_t|p_{(t-m)qL}^{tqL},\boldsymbol{a}_{t-m}^t) \end{aligned} \tag{3.7}$$

and then the detection problem becomes

$$\begin{aligned} \hat{\boldsymbol{a}}_0^{N-1} &= \arg\max_{a_0^{N-1}} f\left(\boldsymbol{y}_0^{N-1}|\boldsymbol{a}_0^{N-1}\right) \\ &= \arg\max_{a_0^{N-1}} f(\boldsymbol{y}_0|a_0)\prod_{t=1}^{N-1} f(\boldsymbol{y}_t|p_{(t-m)qL}^{tqL},\boldsymbol{a}_{t-m}^t) \end{aligned} \tag{3.8}$$

Since the additive white Gaussian noise $w[n], n = 1, \cdots, NqL$ is independent, identically distributed (i.i.d.) and follows a normal distribution with zero mean and variance being σ^2, $\bar{w}_t = \left[w[tqL+1], \cdots, w[(t+1)qL]\right]^T$ follows a multivariate normal distribution with qL-dimensional mean vector $\mathbf{0}$ and $qL \times qL$ covariance matrix $\Sigma = \sigma^2\mathbf{I}$.

Given $p_{(t-m)qL}^{tqL}$ and $\boldsymbol{a}_{t-m}^t$, $\boldsymbol{p}_t$ can be obtained by equation (2.6a). And we know that $\boldsymbol{p}_t$ is the mean of $\boldsymbol{y}_t$. So, the conditional pdf of $\boldsymbol{y}_t$ given $p_{(t-m)qL}^{tqL}$ and $\boldsymbol{a}_{t-m}^t$ is the same

with the conditional pdf of $\boldsymbol{y}_t$ given $\boldsymbol{p}_t$. Moreover, we can conclude that

$$f(\boldsymbol{y}_t|p_{(t-m)qL}^{tqL}, \boldsymbol{a}_{t-m}^{t}) = f(\boldsymbol{y}_t|\boldsymbol{p}_t) \tag{3.9}$$

$$= \frac{1}{(2\pi\sigma^2)^{qL/2}} \exp\big(-\frac{(\boldsymbol{y}_t-\boldsymbol{p}_t)^T(\boldsymbol{y}_t-\boldsymbol{p}_t)}{2\sigma^2}\big)$$

$$= \frac{1}{(2\pi\sigma^2)^{qL/2}} \exp\big(-\frac{\sum_{n=tqL+1}^{(t+1)qL}(y[n]-p[n])^2}{2\sigma^2}\big) \tag{3.10}$$

where $\boldsymbol{p}_t$ depends on $p_{(t-m)qL}^{tqL}$ and $\boldsymbol{a}_{t-m}^{t}$. In order to make the following expression easy to understand, we define $\boldsymbol{a}_{t-m}^{t}$ as a state with notation $\bar{S}_t$. And the length of each state is $m+1$.

Here, we assume that the initial value $p[0]$ is 0. Given $p[0]$ and a_0, we can compute the vector $\boldsymbol{p}_0$ iteratively with equation (2.6a). So, the conditional pdf of $\boldsymbol{y}_0$ given a_0 is given by,

$$f(\boldsymbol{y}_0|a_0) = \frac{1}{(2\pi\sigma^2)^{qL/2}} \exp\big(-\frac{\sum_{n=0}^{qL}(y[n]-p[n])^2}{2\sigma^2}\big). \tag{3.11}$$

By combining function (3.10) and (3.11), the ML sequence estimation of the input sequence $\boldsymbol{a}$ is achieved,

$$\hat{\boldsymbol{a}}_0^{N-1} = \arg\max_{\boldsymbol{a}_0^{N-1}} f(\boldsymbol{y}_0|a_0) \prod_{t=1}^{N-1} f(\boldsymbol{y}_t|p_{(t-m)qL}^{tqL}, \boldsymbol{a}_{t-m}^{t})$$

$$= \arg\max_{\boldsymbol{a}_0^{N-1}} \prod_{t=0}^{N-1} \frac{1}{(2\pi\sigma^2)^{qL/2}} \exp\big(-\frac{\sum_{n=tqL+1}^{(t+1)qL}(y[n]-p[n])^2}{2\sigma^2}\big) \tag{3.12}$$

$$= \arg\min_{\boldsymbol{a}_0^{N-1}} \sum_{t=0}^{N-1} \{ \sum_{n=tqL+1}^{(t+1)qL} (y[n]-p[n])^2 \} \tag{3.13}$$

As we mentioned above, we know that $p[n]$, for $n = tqL+1, \cdots, (t+1)qL$, depends on the state $S_t = \boldsymbol{a}_{t-m}^{t}$ and $p_{(t-m)qL}^{tqL}$. Thus, the value of $\sum_{n=tqL+1}^{(t+1)qL}(y[n]-p[n])^2$ is also determined by S_t and $p_{(t-m)qL}^{tqL}$. If $p_{(t-m)qL}^{tqL}$ don't depend on the past $\boldsymbol{a}$, we can use Viterbi algorithm to recover the input sequence perfectly. But in this feedback system, the past $\boldsymbol{p}$ always affect its following $\boldsymbol{p}$. Therefore, it is hard to obtain an optimal estimation of the input sequence $\boldsymbol{a}$ with the Viterbi algorithm. So, a greedy algorithm inspired by Viterbi algorithm is proposed in our work.

In the our proposed algorithm, we still use S_t to denote a state. Since the length of S_t is $m+1$, there are 3^{m+1} metric paths. In order to make the estimation tractable, we assume that Assumption 2 holds and generate $p^{kqL}_{(k-m)qL}, k = 0, 1, \cdots, N-1$ in the process of decoding $\boldsymbol{a}$. Suppose that we have reached the k-the feature. We assume that there is only one surviving path for each state at the $k-1$-th stage. m

Assumption 2 *At the $(k-1)-th$ input feature, the surviving path ($\tilde{\boldsymbol{a}}_0^{k-1}$) for each state S_{k-1} is optimal.*

And then given $\tilde{\boldsymbol{a}}_0^{k-1}$, $p^{kqL}_{(k-m)qL}$can be computed for each state. In the trellis graph, from state S_{k-1} to state S_k, we can generate $\boldsymbol{p}_k$ for each possible state S_k. And then we pick the best state and its corresponding $p^{kqL}_{(k-m)qL}$. With this scheme, the estimation of input sequence $\boldsymbol{a}$ becomes tractable.

To explain how we implement the Viterbi algorithm, we start with function (3.7), which is

$$\begin{aligned} & f(\boldsymbol{y}_0|a_0)\prod_{t=1}^{N-1} f(\boldsymbol{y}_t|p^{tqL}_{(t-m)qL}, \boldsymbol{a}^t_{t-m}) \\ & \quad = [(\boldsymbol{y}_0|a_0)\prod_{t=1}^{N-2} f(\boldsymbol{y}_t|p^{tqL}_{(t-m)qL}, \boldsymbol{a}^t_{t-m})] f(\boldsymbol{y}_{N-1}|p^{(N-1)qL}_{(N-1-m)qL}, \boldsymbol{a}^{N-1}_{N-1-m}) \end{aligned} \quad (3.14)$$

Let $\varphi(a_0^k) = f(\boldsymbol{y}_0|a_0)\prod_{t=1}^{k} f(\boldsymbol{y}_t|p^{tqL}_{(t-m)qL}, \boldsymbol{a}^t_{t-m})$, $\beta(a^k_{k-m}) = f(\boldsymbol{y}_k|p^{kqL}_{(k-m)qL}, \boldsymbol{a}^k_{k-m})$ and $\beta(S_k) = \beta(a^k_{k-m})$, we have

$$\varphi(a_0^k) = \varphi(a_0^{k-1})\beta(S_k) \quad (3.15)$$

and also let $\Phi(a_0^m) = \varphi(a_0^m)$. So the decoding strategy of Viterbi algorithm for the certain $k-th$ state is

$$\Phi(a^k_{k-m}) = \min_{a_{k-m-1}=0,1,2} \Phi(a^{k-1}_{k-m-1})\beta(S_k), k = m+1, \cdots, N-1 \quad (3.16)$$

In Given the Assumption 2, it is obviously that the estimation sequence $\hat{\tilde{a}}_0^{N-1}$ obtained by function (3.16) is the exactly sequence that we want by minimizing function (3.15).

In the process of computing function (3.16), because of given $S_k = a_{k-m}^{k}$, three different states of $S_{k-1} = a_{k-m-1}^{k-1} \in \{0a_{k-m} \cdots a_{k-1}, 1a_{k-m} \cdots a_{k-1}, 2a_{k-m} \cdots a_{k-1}\}$ exist. And for each state S_{k-1}, there is a surviving path $\tilde{\boldsymbol{a}}_0^{k-1}$ which is used to compute its corresponding p_0^{kqL}. Besides, $p_{kqL+1}^{(k+1)qL}$ can also be obtained as a_k and p_0^{kqL} is given. Finally, $\Phi(a_{k-m}^{k})$ can be computed for each $k \in m+1, \cdots, N-1$.

To assess the performance of the proposed algorithm, we use a genie-aided detector to determine a lower bound of FER. The lower bound provides a benchmark which is the best result that is achievable. For the genie-aided detector, instead of making an assumption and computing $\boldsymbol{p}$ step by step, we use the true $\boldsymbol{p}$ generated by the simulation model. For example, when we are decoding the k-th state S_k, the $p_{(k-m)qL}^{kqL}$ are real values which are established by simulation model. And then $p_{kqL+1}^{(k+1)qL}$ is computed with real $p_{(k-m)qL}^{kqL}$ and fixed S_k.

By comparing the performance of our algorithm with this lower bound, we can establish that our proposed algorithm exhibits good performance.

CHAPTER 4. SIMULATION EXPERIMENT AND RESULT

In this section, we assess the performance of the proposed algorithm. The data for evaluation is generated by a `Simulink` model. In the part of the nonlinear tip-media interaction force, we have $\theta = 0.01, \lambda = 0.1$, $\delta = -0.6$, and the precise form for $\phi(p)$ is

$$\phi(p) = 0.02\Big[(\mathrm{e}^{-(p+0.6)/0.1} - \frac{1}{2})^2 - \frac{1}{4}\Big] \tag{4.1}$$

We also set the first resonant frequency of the cantilever and quality factor as

$$f_c = 2.947 \times 10^5 \qquad Q = 50. \tag{4.2}$$

And the sampling period of this system is $T_s = T_c/L$ with $L = 120$, where $T_c = 1/f_c$. Although higher sampling rate reduces the error between the discrete and continuous system, it demands more computational burden and memory. So we have to balance between accuracy and speed. Here, we find that $L = 120$ is a good choice that makes the balance. We show in Fig. 4.1 the impulse response, $\Gamma(t)$ which satisfies the Assumption 1. And we can conclude that the length of the channel impulse response is approximately 60 $(60 * T_c)$.

We compare two different choices of the number of cantilever hits, q, in every feature duration T:

$$(q, m) = (60, 1) \qquad \text{and} \qquad (q, m) = (30, 2) \tag{4.3}$$

The larger the m is, the more severe the inter-symbol-interference (ISI) is. For the dither forcing, its amplitude A is set to 0.007. And then if $z(t) = 0$ which indicates that there is no tip-media interaction, the amplitude of $p(t)$ is about 0.7. Here, the sample has

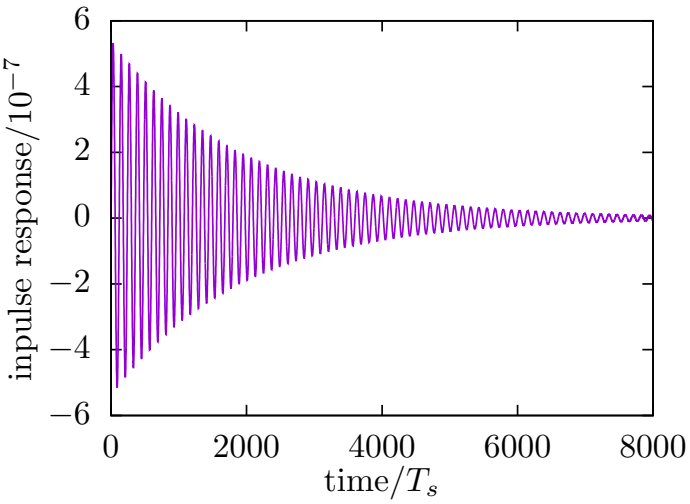

Figure 4.1: Channel impulse response.

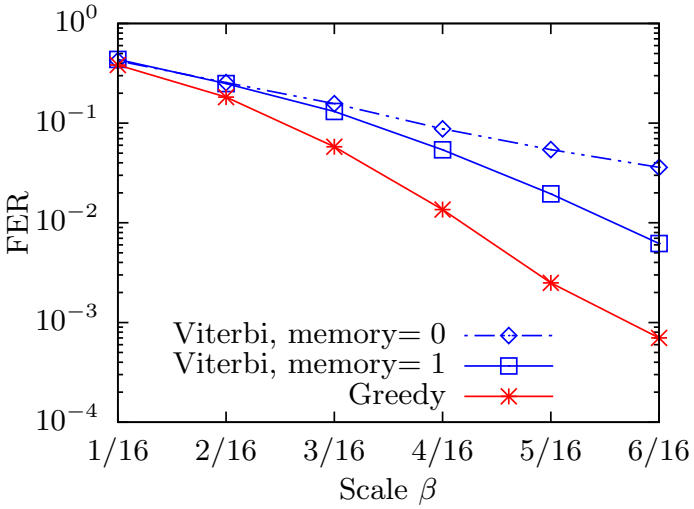

Figure 4.2: At $m = 1$, compare the FER for Greedy and Viterbi with different interaction length $(0, 0.05\beta, 0.1\beta)$ where β varies from $\frac{1}{16}$ to $\frac{6}{16}$ with step $\frac{1}{16}$.

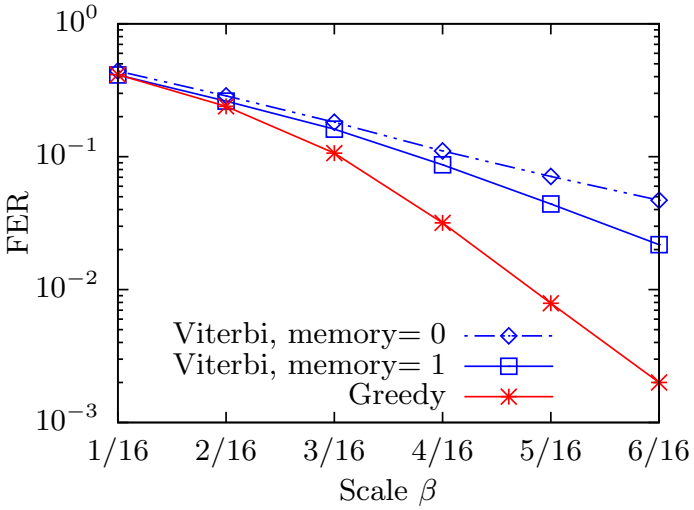

Figure 4.3: At $m = 2$, compare the FER for Greedy and Viterbi with different interaction length $(0, 0.05\beta, 0.1\beta)$ where β varies from $\frac{1}{16}$ to $\frac{6}{16}$ with step $\frac{1}{16}$.

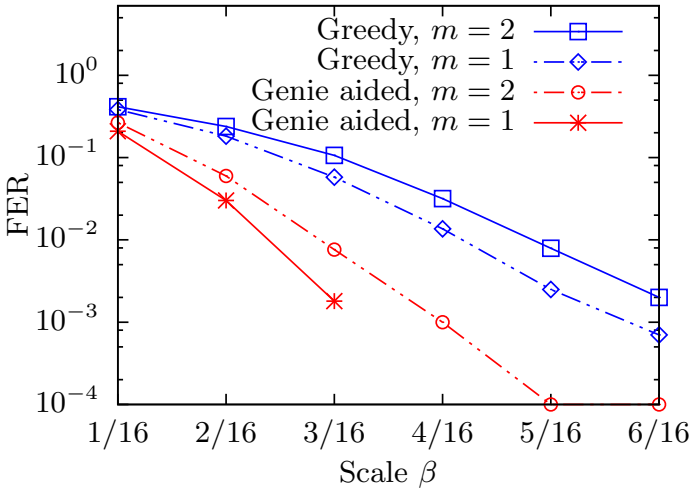

Figure 4.4: The lower bound obtained by a genie-aided detector.

three different height which is determined by B. In order to evaluate the performance, our experiment is conducted in various interaction lengths. Different interaction lengths imply different signal to noise ratio (SNR). In this paper, we demonstrate the performance for the different interaction lengths by $B = 0.05\beta$, where the scale β varies among $\{\frac{1}{16}, \frac{2}{16}, \frac{3}{16}, \frac{4}{16}, \frac{5}{16}, \frac{6}{16}\}$. The height of sample profile with feature 0 is assumed to be 0, i.e., the cantilever initially oscillates freely in air. With fixed B, the height of sample profile with feature 1 is 0.05β and the height of sample profile with feature 2 is 0.1β. The tip-media interaction exists in feature 1 and feature 2. Moreover, the power of the measurement noise is set to 0.1946.

We take into account two kinds of ISI via two different values for m, 1 and 2, which are shown in Fig. 4.2 and Fig. 4.3, respectively. Fig. 4.2 and Fig. 4.3 compare the FER of two different detectors at different interaction length. Both figures show that the proposed algorithm outperforms the Viterbi algorithm in three-level samples detection. For Viterbi algorithm with the scheme proposed by Kumar *et al.*, we choose two system memories which are $memory = 0$ and $memory = 1$.

Furthermore, we give a lower bound for the greedy algorithm. The results of the lower bound FER are shown on Fig. 4.4. While the lower bound is not achievable, it provides us with a baseline that we can compare against.

CHAPTER 5. CONCLUSIONS AND FUTURE WORK

In this work we have presented a sequence detection algorithm that helps to resolve three different topographic levels in dynamic mode AFM imaging. Our initial investigation showed that a previously proposed two-level imaging algorithm had a rapid degradation in performance when considering three-level imaging. Accordingly, we considered a setup where somewhat more information is known to us. Specifically, we assumed that the parameters of the nonlinear tip-media interaction were available to us. Even in this scenario, feature detection is quite challenging. We proposed a suboptimal Viterbi-like algorithm that exhibits performance and compared it a lower bound that was derived based on assuming a genie-aided detector.

Future work will include performing a careful study of extending this approach to even more levels and considering different tip-media interaction force profiles.

REFERENCES

[1] G. Binnig, C. F. Quate, and C. Gerber, "Atomic force microscope," *Phys. Rev. Lett.*, vol. 56, no. 9, p. 930, 1986.

[2] S. Ghosal, G. Saraswat, A. Ramamoorthy, and M. Salapaka, "Topography detection using innovations mismatch method for high speed and high density dynamic mode afm," in *Amer. Contr. Conf.*, IEEE, 2013, pp. 5500–5505.

[3] A. Sebastian, M. Salapaka, D. Chen, and J. Cleveland, "Harmonic and power balance tools for tapping-mode atomic force microscope," *J. Appl. Phys.*, vol. 89, no. 11, pp. 6473–6480, 2001.

[4] N. Kumar, P. Agarwal, A. Ramamoorthy, and M. V. Salapaka, "Maximum-likelihood sequence detector for dynamic mode high density probe storage," *IEEE Trans. Commun.*, vol. 58, no. 6, pp. 1686–1694, 2010.

[5] L. Wasserman, *All of statistics: A concise course in statistical inference*. Springer, 2004.